

## Inhibition of Hydroxyapatite Formation in Aqueous Solutions by Zinc and 1,2-Dihydroxy-1,2-bis(dihydroxyphosphonyl)ethane

Maria Dalpi, Eleni Karayianni and Petros G. Koutsoukos\*

*Institute of Chemical Engineering and High Temperature Chemical Processes P.O. Box 1414, Patras, Greece and Department of Chemical Engineering, University of Patras GR-26500, Patras, Greece*

The kinetics of crystal growth of hydroxyapatite [ $\text{Ca}_5(\text{PO}_4)_3\text{OH}$ , HAP], the thermodynamically most stable calcium phosphate phase, at 37 °C, pH 7.4 and ionic strength 0.1 mol dm<sup>-3</sup> has been investigated. The kinetics results showed a surface-controlled spiral growth mechanism. The presence of 1,2-dihydroxy-1,2-bis(dihydroxyphosphonyl)ethane (DDPE) and Zn strongly inhibited the crystal growth of HAP. The kinetics results in the presence of each of the two inhibitors supported the suggestion that they act through adsorption and subsequent blocking of the active growth sites of the HAP seed crystals. The affinity found both for DDPE and Zn for the HAP substrate was higher by up to three orders of magnitude than the affinities reported in the literature for a number of inhibitors. In solutions in which both inhibitors existed simultaneously no synergism was found. The inhibition caused by the presence of Zn was stronger compared with that caused by DDPE, which inhibited the crystal growth of HAP more drastically as the solution supersaturation increased.

Phosphorus-containing compounds are extensively used as inhibitors for the control of corrosion in water pipes, boilers, cooling towers *etc.*<sup>1-7</sup> However, degradation of these compounds in aquatic systems may lead to the release of inorganic orthophosphate and subsequently to the formation of very hard deposits consisting mainly of calcium phosphate salts.<sup>8</sup> Depending on the solution pH and on the concentration levels of calcium and phosphate in water, a number of phases may be formed. The calcium phosphate phases which may be formed at relatively low temperature (< 100 °C) and pressures (1 atm) in water are, in order of decreasing solubility, calcium phosphate dihydrate ( $\text{CaHPO}_4 \cdot 2\text{H}_2\text{O}$ , DCPD), octacalcium phosphate [ $\text{Ca}_8\text{H}_2(\text{PO}_4)_3 \cdot 2.5\text{H}_2\text{O}$ , OCP] and hydroxyapatite [ $\text{Ca}_5(\text{PO}_4)_3\text{OH}$ , HAP]. According to thermodynamics, the formation of HAP (which is the least soluble) is favoured. In natural waters, or in waters used in industrial applications, the relatively higher pH (7.0-8.0) accelerates the conversion of any unstable phase which may be formed to HAP. As a result, calcium phosphate deposits are found to consist mainly of HAP. Moreover, since both the free calcium and phosphate levels are quite low, it is possible that the formation of scale occurs directly onto the heated surfaces, without the mediation of precursor phases.

Since HAP formation is a problem in a number of industrial operations, efforts have been focused on the investigation of various water additives which may retard or even eliminate the formation of this salt. Phosphonates have been shown to be a successful class of inhibitors<sup>9-11</sup> and have been commercialized mainly because of their superior stability towards thermal decomposition, in comparison with the pyrophosphates<sup>12</sup> or the polyphosphates.<sup>13</sup> However, even the chemically resistant P-C-P bond of the diphosphonates is degraded after prolonged use in heated waters. In the present work, we have examined the effect of an organophosphorus compound, namely 1,2-dihydroxy-1,2-bis(dihydroxyphosphonyl)ethane (DDPE).

The synthesis of DDPE has been described elsewhere.<sup>14</sup> The main advantage of DDPE is its stability at elevated temperatures and it has been suggested for use as a fire retardant in textiles. The compound was tested by batch crystallization experiments at conditions of constant solution supersaturation.<sup>15</sup> There are reports in the literature that the combination of more than one inhibitor may yield enhanced inhibition in water-formed scale deposits.<sup>8</sup> In this case, the combined effect, known as the synergistic effect, is stronger

than using each of the inhibitors separately. Since zinc is widely used for the protection of metal parts, we have further examined the effect of this metal ion on the formation of HAP and the possibility of a synergistic effect of  $\text{Zn}^{2+}$  in combination with DDPE.

### Experimental

All experiments were performed at  $37.0 \pm 0.1$  °C in a thermostatted double-walled, water-jacketed Pyrex glass reactor (volume 0.06 dm<sup>3</sup>). Calcium nitrate, potassium dihydrogen phosphate and potassium nitrate stock solutions were prepared from the respective crystalline solids (Analytical Grade, Fluka AG) using triply distilled, CO<sub>2</sub>-free water. Standardization of the stock solutions was achieved *via* potentiometric and spectrophotometric titrations as described elsewhere.<sup>15,16</sup> The pH measurements were made using glass/saturated calomel electrodes (Radiometer G202C and K402, respectively) standardized before and after each experiment with NBS standard buffer solutions.<sup>16</sup> HAP seed crystals were prepared from concentrated calcium nitrate and potassium phosphate as detailed elsewhere.<sup>17</sup> The seed crystals were aged for three years in the mother liquor. Next, the suspension was filtered through membrane filters (Millipore 0.22 μm), washed with hot distilled water (70 °C) and dried at 105 °C for 12 h. The seed crystals were kept in a dessicator for subsequent use. The specific surface area of the dried crystals was measured by a multiple-point BET method (Perkin Elmer Sorptometer, Model 212 D) and was found to be 27.0 m<sup>2</sup> g<sup>-1</sup>. Powder X-ray diffractograms of the seed crystals (Philips XRG 3000) showed that they consisted exclusively of HAP. Chemical analysis following the dissolution of solid samples gave a molar ratio of total calcium ( $[\text{Ca}]_0$ ) to total phosphate ( $[\text{P}]_0$ ) of  $1.67 \pm 0.02$ . The experiments were performed at sustained supersaturation<sup>15</sup> at constant ionic strength, 0.1 mol dm<sup>-3</sup>, adjusted with potassium nitrate. The supersaturated solutions were prepared in the glass reactor by mixing equal volumes (0.025 dm<sup>3</sup> each) of calcium nitrate and potassium dihydrogen phosphate. The ionic strength of each of the solutions was adjusted to 0.1 mol dm<sup>-3</sup> by the addition of the required amount of the stock potassium nitrate solution. The solution pH was adjusted to 7.40 by the slow addition of standard potassium hydroxide solution (Merck Titrisol). Throughout the course of precipitation and during the pH adjustment of the solutions, water vapour

saturated nitrogen (Linde Hellas, 99.99%) was bubbled through the solution. All solutions were stable with respect to spontaneous precipitation for time periods exceeding 48 h. After the pH adjustment, a further waiting period of ca. 3 h was allowed to ensure equilibration. Next, a weighted amount of the HAP seed crystals was added to the solution. Seeding of the supersaturated solutions resulted in a pH drop of the solution because of the crystal growth of the added crystallites. A pH drop as small as 0.005 pH units triggered the addition of titrants from the two mechanically coupled burettes of an appropriately modified automatic titrator (Radiometer TTT1b, ABU 1, SBR2C). The following titrant concentrations were used: burette 1, total calcium,  $[Ca]_v/mol\ dm^{-3} = 10x + 2x$ , total potassium nitrate/mol  $dm^{-3} = 2(0.1 - 10x)$ ; burette 2, total phosphate,  $[P]_v/mol\ dm^{-3} = (3/5)(10x) + 2y$ , total KOH/mol  $dm^{-3} = (1/5)(10x) + 2[(3/5)(10x)] + 2z$ , where  $x$ ,  $y$  and  $z$  are, respectively, the concentrations of total calcium, total phosphate (as  $KH_2PO_4$ ) and of the total base (KOH) added for pH adjustment in the working supersaturated solution. In experiments in which DDPE was used, twice the concentration of this compound in the supersaturated solutions was added in burette 2 in order to avoid dilution of this compound owing to the addition of the titrant solutions. In the investigation of the  $Zn^{2+}$  ions, the metal ions (two times their concentration in the working solution) were included in burette 1, in order to avoid zinc phosphate spontaneous precipitation. During the course of the precipitation process, samples were withdrawn and the aqueous phase was analysed for calcium and phosphorus<sup>17</sup> in order to verify the constancy of the solution composition. In all cases, the concentrations remained constant throughout the course of the precipitation process to within  $\pm 2-3\%$ .

## Results and Discussion

The driving force for the crystal growth process is the difference in chemical potential,  $\Delta\mu$ , between the crystalline and aqueous state of HAP, *i.e.*:<sup>18</sup>

$$\Delta\mu = \mu_{HAP(s)} - \mu_{HAP(aq)} \quad (1)$$

For

$$\mu_{HAP} = \mu_{HAP}^0 + \frac{RT}{9} \ln \alpha_{Ca^{2+}}^5 \alpha_{PO_4^{3-}}^3 \alpha_{OH^-} \quad (2)$$

where  $\alpha_{Ca^{2+}}$ ,  $\alpha_{PO_4^{3-}}$  and  $\alpha_{OH^-}$  are the activities of  $Ca^{2+}$ ,  $PO_4^{3-}$  and  $OH^-$  ions, respectively. Taking the difference of the chemical potentials in the aqueous and the crystalline state we have:

$$\Delta\mu = \frac{RT}{9} \ln \frac{[\alpha_{Ca^{2+}(aq)}]^5 [\alpha_{PO_4^{3-}(aq)}]^3 [\alpha_{OH(aq)}]}{\alpha_{Ca(s)}^5 \alpha_{PO_4(s)}^3 \alpha_{OH(s)}} \quad (3)$$

or

$$\Delta\mu = \frac{RT}{9} \ln \frac{K_s}{K_s^0} = \frac{RT}{9} \ln \Omega \quad (4)$$

where  $R$  is the gas constant,  $T$  the absolute temperature and  $K_s$  and  $K_s^0$  the ionic products of HAP in solution and at equilibrium, respectively. The ionic product of the supersaturated solutions was computed taking into account the equilibria and the constants summarized in Table 1. The computation of the solution speciation involved also the charge and mass balance equations with successive approximations for the solution ionic strength using the Davies formulation for the activity coefficients.<sup>19</sup> The rates of crystallization of HAP were found to depend on the relative solution supersaturation,  $\sigma$ , with respect to HAP defined in

**Table 1** Equilibria involved in the computation of the solution speciation

equilibrium	log K (1 atm, ionic strength 0)
$H^+ + PO_4^{3-} = HPO_4^{2-}$	12.18 <sup>a</sup>
$H^+ + HPO_4^{2-} = H_2PO_4^-$	7.25 <sup>a</sup>
$H^+ + H_2PO_4^- = H_3PO_4$	2.21 <sup>a</sup>
$Ca^{2+} + PO_4^{3-} = CaPO_4$	6.54 <sup>a</sup>
$Ca^{2+} + HPO_4^{2-} = CaHPO_4^0$	1.50 <sup>a</sup>
$Ca^{2+} + H_2PO_4^- = CaH_2PO_4^+$	2.83 <sup>a</sup>
$Zn^{2+} + HPO_4^{2-} = ZnHPO_4$	5.03 <sup>b</sup>
$Zn^{2+} + H_2PO_4^- = ZnH_2PO_4^+$	1.20 <sup>b</sup>
$Zn^{2+} + OH^- = ZnOH^+$	5.00 <sup>b</sup>
$Ca^{2+} + OH^- = CaOH^+$	1.81 <sup>a</sup>
$Zn^{2+} + 2OH^- = Zn(OH)_2^0$	11.10 <sup>b</sup>
$Zn^{2+} + 3OH^- = Zn(OH)_3^-$	13.60 <sup>b</sup>
$Zn^{2+} + 4OH^- = Zn(OH)_4^{2-}$	14.80 <sup>b</sup>
$2Zn^{2+} + OH^- = Zn_2OH^{3+}$	5.00 <sup>b</sup>
$H^+ + A^{4-} = HA^{3-}$	9.34 <sup>c</sup>
$H^+ + HA^{3-} = H_2A^{2-}$	6.60 <sup>c</sup>
$H^+ + H_2A^{2-} = H_3A^-$	6.60 <sup>c</sup>
$H^+ + H_3A^- = H_4A$	3.50 <sup>c</sup>
$Ca^{2+} + H_2A^{2-} = CaH_2A^0$	2.96 <sup>c</sup>
$Zn^{2+} + 2OH^- = Zn(OH)_2(s)$	-15.52 <sup>b</sup>
$5Ca^{2+} + 3PO_4^{3-} + OH^- = Ca_5(PO_4)_3OH(s)$	-58.62 <sup>d</sup>
$3Zn^{2+} + 2PO_4^{3-} = Zn_3(PO_4)_2(s)$	-35.3 <sup>b</sup>

<sup>a</sup> M. Hamad and J. C. Heughebaert, *J. Cryst. Growth*, 1986, **79**, 192;

<sup>b</sup> R. M. Smith and A. E. Martell, *Critical Stability Constants*, Plenum Press, New York, 1976, vol. 4; <sup>c</sup> A. Xyla, J. Mikroyannidis and P. G. Koutsoukos, *J. Colloid Interface Sci.*, 1992, **153**, 537; <sup>d</sup> M. H. Salimi, J. C. Heughebaert and G. H. Nancollas, *Langmuir*, 1985, **1**, 119; Note  $H_4A$  stands for DDPE.

eqn. (5):

$$\sigma = \frac{(K_s)^{1/9} - (K_s^0)^{1/9}}{(K_s^0)^{1/9}} = \Omega^{1/9} - 1 \quad (5)$$

In eqn. (5),  $\Omega$  is the saturation ratio of the solution with respect to HAP and  $K_s^0$  the corresponding thermodynamic solubility product. The initial experimental conditions and the experimentally measured rates of crystallization are summarized in Table 2. In all cases, HAP was formed exclusively as was verified both by powder X-ray diffraction of the reaction products and also as predicted by the calculations of the thermodynamic driving force. The thermodynamic calculations showed that the presence of the inhibitors at the concentration levels used in our experiments did not influence the relative solution supersaturation with respect to HAP. As may be seen from the experimental results, the rates of crystallization were higher the higher the solution supersaturation. The kinetics data were fitted to eqn. (6):<sup>20,21</sup>

$$R_g = ks\sigma^n \quad (6)$$

where  $R_g$  is the crystal growth rate,  $k$  the rate constant,  $s$  a function of the number of the active growth sites provided by the substrate (seed crystals), and  $n$  the apparent order of the crystallization process. Logarithmic plots according to eqn. (6) are shown in Fig. 1. From the linear plot obtained, a value of  $n = 2.00 \pm 0.30$  was found, suggesting a surface-controlled spiral growth mechanism. When DDPE or Zn were present in the supersaturated solutions, the rate of HAP crystal growth decreased significantly. The rate of decrease is shown in Fig. 2, in which the amount of HAP (in moles) grown on the seed crystal after 1 h as a function of DDPE and Zn is plotted. As may be seen, the presence of Zn resulted in a more drastic decrease of the rate of HAP crystal growth.

The presence of foreign compounds or ions in the supersaturated solutions in which the HAP growth takes place results in the interaction of the solid precipitate with the

**Table 2** Experimental conditions, relative supersaturation and measured rates of crystal growth of HAP seed crystals; 37 °C, pH 7.40, ionic strength = 0.1 mol dm<sup>-3</sup> in KNO<sub>3</sub>

exp. no.	[Ca] <sub>t</sub> /10 <sup>-4</sup> mol dm <sup>-3</sup>	[P] <sub>t</sub> /10 <sup>-4</sup> mol dm <sup>-3</sup>	[DDPE]/10 <sup>-8</sup> mol dm <sup>-3</sup>	[Zn]/10 <sup>-8</sup> mol dm <sup>-3</sup>	σ <sub>HAP</sub>	R/10 <sup>-9</sup> mol m <sup>-2</sup> min <sup>-1</sup>
1110	4.00	2.40	—	—	6.80	19.5
1120	3.00	1.80	—	—	5.82	11.7
1130	2.00	1.20	—	—	4.43	6.0
1140	1.00	1.00	—	—	2.70	2.0
1150	1.00	0.60	—	—	2.04	0.8
1111	4.00	2.40	1.0	—	6.80	8.3
1112	4.00	2.40	5.0	—	6.80	7.9
1113	4.00	2.40	10.0	—	6.80	2.8
1114	4.00	2.40	50.0	—	6.80	1.7
1115	4.00	2.40	100.0	—	6.79	0.9
1161	3.00	1.80	50.0	—	5.82	3.1
1162	2.00	1.20	50.0	—	4.43	2.9
1163	1.00	0.60	50.0	—	2.04	2.1
1116	4.00	2.40	700.0	—	6.79	—
1121	4.00	2.40	—	1.0	6.80	3.0
1122	4.00	2.40	—	5.0	6.80	2.6
1123	4.00	2.40	—	10.0	6.80	1.7
1124	4.00	2.40	—	50.0	6.80	0.9
1125	4.00	2.40	—	70.0	6.80	0.7
1131	4.00	2.40	1.0	1.0	6.80	9.0
1132	4.00	2.40	10.0	1.0	6.80	8.0

σ<sub>HAP</sub>: relative supersaturation with respect to HAP; [Ca]<sub>t</sub>: total calcium; [P]<sub>t</sub>: total phosphate.

solute species. When the solute species contain functional groups such as, *e.g.*, hydroxyl or carboxylate they are adsorbed reversibly from hydrogen-bonding solvents and the Langmuir formalism may describe the solid-solute inter-

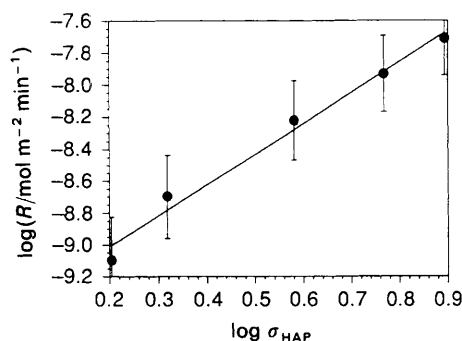


**Fig. 1** Kinetics of HAP crystal growth at constant supersaturation. pH 7.40, 37 °C, 0.1 mol dm<sup>-3</sup> KNO<sub>3</sub>. Dependence of the rates of crystal growth of HAP on the relative solution supersaturation with respect to HAP.

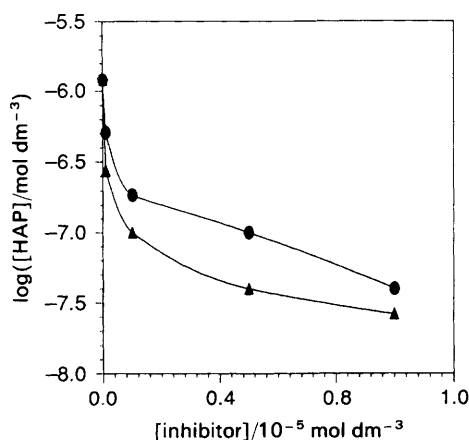


**Fig. 2** Inhibition of the crystal growth of HAP at conditions of sustained supersaturation. Plot of the number of moles of HAP formed in 1 h of growth in the presence of: (○) DDPE; (△) Zn. [Ca]<sub>t</sub> = 4.0 × 10<sup>-4</sup> mol dm<sup>-3</sup>; [P]<sub>t</sub> = 2.4 × 10<sup>-4</sup> mol dm<sup>-3</sup>; pH 7.40, 37 °C, 0.1 mol dm<sup>-3</sup> KNO<sub>3</sub>

action.<sup>22</sup> The positively charged metal ions (including their charged complexes in aqueous medium) are expected to interact with the HAP surface, negatively charged at pH 7.40.<sup>23</sup> Assuming that the additives are adsorbed onto the HAP seed crystals according to the simple Langmuir model, occupying a fraction,  $\theta$ , of the active growth sites ( $0 < \theta < 1$ ), the rates of HAP crystal growth in their presence,  $R_i$ , are given by:<sup>15,24</sup>

$$R_i = R_0(1 - \theta) \quad (7)$$

where  $R_0$  is the crystallization rate in the absence of inhibitors. According to the Langmuir isotherm:

$$1 - \theta = \frac{1}{1 + K_L C_i} \quad (8)$$

In eqn. (8),  $K_L$  is a measure of the affinity of the adsorbate for the adsorbent and  $C_i$  is the concentration (total) of the additive.<sup>25</sup> Combination of eqn. (7) and (8) yields:<sup>26</sup>

$$\frac{R_0}{R_i} = 1 + K_L C_i \quad (9)$$

Plots of the ratio  $R_0/R_i$  as a function of  $C_i$  are shown in Fig. 3 and 4 for DDPE and Zn, respectively. The linear fit of the kinetics data suggested that for the concentration range investigated, the inhibitory activity for DDPE and Zn may be explained by blocking of the active growth sites by adsorption. The slope of the lines obtained from the fit according to eqn. (9) may be considered as a measure of the affinity of the adsorbate for the substrate. The values of the affinities obtained for DDPE and Zn are very similar and one to three orders of magnitude higher than those corresponding to other HAP inhibitors, as may be seen in the values summarized in Table 3. The higher affinity of Zn for HAP corresponds to the more significant effect of this cation on the rate of HAP crystal growth.

Note that DDPE was found to inhibit the formation of calcium carbonate<sup>27,28</sup> and combination with Zn yielded enhanced inhibition. This case of synergism was investigated for HAP as well. The kinetics results summarized in Table 1, however, showed that the combination of DDPE with Zn gave rates corresponding to those of DDPE alone. The inhibition of HAP crystal growth by DDPE increased with the

**Table 3** Comparative data of affinities of various inhibitors of HAP crystal growth

inhibitor	$10^7 K_L$	ref.
sodium pyrophosphate	0.02	<sup>a</sup>
aminotris(methylenephosphonic acid)	0.06	<sup>a</sup>
1-hydroxyethylidene-1,1-diphosphonic acid	0.13	<sup>a</sup>
1-hydroxyethylidene-1,1-diphosphonic acid	0.21	<sup>b</sup>
ethylenediaminetetrakis(methylenephosphonic acid)	0.81	<sup>a</sup>
hexamethylenediaminetetrakis(methylenephosphonic acid)	0.14	<sup>a</sup>
citric acid	0.002	<sup>a</sup>
mellitic acid	0.16	<sup>b</sup>
1,2-dihydroxy-1,2-bis(dihydroxyphosphonyl)ethane	2.16	this work
Zn	3.02	this work

<sup>a</sup> Z. Amjad, *Langmuir*, 1987, **3**, 1063; <sup>b</sup> P. G. Koutsoukos, Z. Amjad and G. H. Nancollas, *J. Colloid Interface Sci.*, 1981, **83**, 599; <sup>c</sup> Z. Amjad, in *Adsorption and Surface Chemistry of Hydroxyapatite*, ed. D. W. Misra, Plenum, New York, 1984.

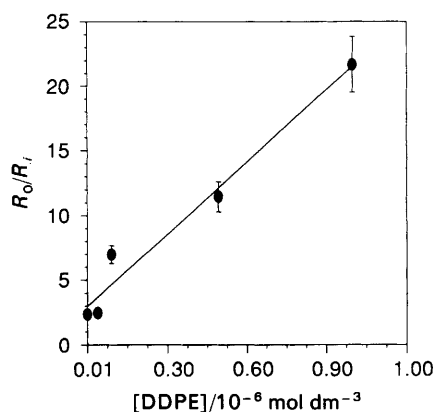


**Fig. 3** Plot of the ratio of the rates of HAP crystal growth in the absence,  $R_0$ , and in the presence,  $R_i$ , of DDPE at constant solution supersaturation.  $[Ca]_i = 4.0 \times 10^{-4} \text{ mol dm}^{-3}$ ;  $[P]_i = 2.4 \times 10^{-4} \text{ mol dm}^{-3}$ ; pH 7.40, 37 °C, 0.1 mol dm<sup>-3</sup> KNO<sub>3</sub>.

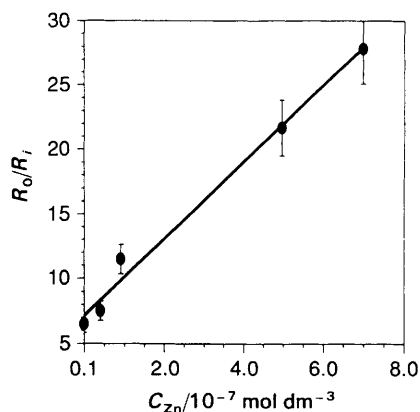


**Fig. 4** Plot of the ratio of the rates of HAP crystal growth in the absence,  $R_0$ , and in the presence,  $R_i$ , of Zn at constant solution supersaturation.  $[Ca]_i = 4.0 \times 10^{-4} \text{ mol dm}^{-3}$ ;  $[P]_i = 2.4 \times 10^{-4} \text{ mol dm}^{-3}$ ; pH 7.40, 37 °C, 0.1 mol dm<sup>-3</sup> KNO<sub>3</sub>.

relative solution supersaturation with respect to HAP, as may be seen in Fig. 5. The reduced effectiveness of DDPE at lower supersaturations may be due to Coulombic interactions which may, in turn, influence the adsorption of DDPE onto the HAP crystallites. Calcium and phosphate are potential-determining ions for HAP and it is therefore anticipated that the surface charge of the growing crystals changes with the solution supersaturation, being higher the higher the solution supersaturation.

The authors wish to express their gratitude to Professor Dr. John Mikroyannidis of the Department of Chemistry of the

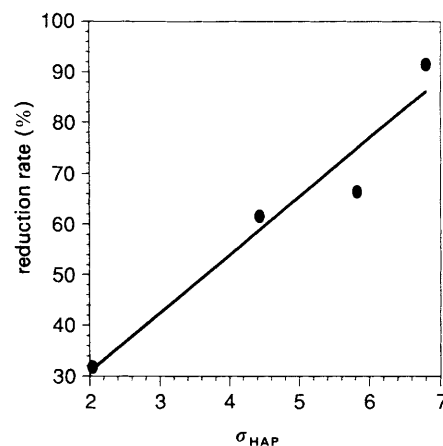


**Fig. 5** Reduction of the crystallization rate of HAP at constant solution supersaturation as a function of the relative supersaturation with respect to HAP in the presence of DDPE; pH 7.40, 37 °C, 0.1 mol dm<sup>-3</sup> KNO<sub>3</sub>,  $[Ca]_i = 4.0 \times 10^{-4} \text{ mol dm}^{-3}$ ;  $[P]_i = 2.4 \times 10^{-4} \text{ mol dm}^{-3}$ ,  $[DDPE] = 5 \times 10^{-7} \text{ mol dm}^{-3}$ .

University of Patras, for providing a pure sample of DDPE. The support of the EEC, contract JOUG-0005C, is also gratefully acknowledged.

## References

- G. B. Hatch, in *Corrosion Inhibitors*, ed. C. C. Nathan, NACE, Houston, Texas, 1973, pp. 113–125.
- G. B. Hatch and O. Rice, *Ind. Eng. Chem.*, 1945, **37**, 710.
- R. W. Zuhl, Z. Amjad and W. F. Hasler, *J. Cooling Tower Inst.*, 1987, **8**, 41.
- G. B. Hatch, *Ind. Eng. Chem.*, 1952, **44**, 1775.
- Z. Amjad, in *Corrosion 1988*, NACE Annual Meeting, March, 1988, St. Louis MI, paper 421.
- E. S. Troscinski and R. G. Watson, *Chem. Eng.*, 1970, 125.
- C. M. Hwa, *Met. Prot. Performance*, 1971, **10**, 24.
- J. C. Cowan and D. J. Weintritt, in *Water Formed Scale Deposits*, Gulf Publ. Co., Houston, Texas, 1976, p. 406.
- G. H. Nancollas and G. L. Gardner, *J. Crystal Growth*, 1974, **21**, 267.
- O. J. Vetter, *J. Petrol. Technol.*, 1972, 977.
- J. L. Meyer and G. H. Nancollas, *Calcif. Tissue Res.*, 1973, **13**, 259.
- J. Green *Ind. Eng. Chem.*, 1950, **42**, 1542.
- P. H. Ralston and S. L. Whitney, *Corrosion/83*, NACE Annual Meeting, San Francisco, 1983, paper 312.
- J. Mikroyannidis, A. K. Tsolis and D. J. Gourghiotis, *Phosphorus and Sulfur*, 1972, **13**, 279.
- P. G. Koutsoukos, Z. Amjad, M. B. Tomson and G. H. Nancollas, *J. Am. Chem. Soc.*, 1980, **102**, 1553.
- E. Dalas and P. G. Koutsoukos, *J. Chem. Soc., Faraday Trans. 1*, 1989, **85**, 3159.
- P. G. Koutsoukos, Ph.D. Thesis, State University of New York, Buffalo, 1980.

- 18 J. Garside, in *Measurement of Crystal Growth Rates*, ed. J. Garside, A. Mersmann and J. Nyvlt, European Federation of Chemical Engineering, Working Party on Crystallization, Munich, Germany, 1990, p. 91.
- 19 G. H. Nancollas, *Interactions in Electrolyte Solutions*, Elsevier, Amsterdam, 1966.
- 20 E. C. Moreno, R. T. Zahradnik, A. Glazman and R. Hwu, *Calcif. Tissue Res.*, 1977, **24**, 47.
- 21 J. P. Barone, G. H. Nancollas and M. B. Tomson, *Calcif. Tissue Res.*, 1976, **21**, 171.
- 22 D. N. Misra, *Langmuir*, 1988, **4**, 953.
- 23 S. J. Zawacki, P. G. Koutsoukos, M. H. Salimi and G. H. Nancollas, in *Geochemical Process at Mineral Surfaces*, ed. J. A. Davies and K. F. Hayes, ACS Symp. Ser. No. 323, American Chemical Society, Washington DC, 1986, pp. 650–662.
- 24 G. Bliznakow, *Fortschr. Min.*, 1958, **36**, 149.
- 25 J. Lyklema, *Fundamentals of Interface and Colloid Science*, Academic Press, London, 1991, vol. 1.
- 26 J. Christoffersen and M. R. Christoffersen, *J. Cryst. Growth*, 1981, **53**, 42.
- 27 P. G. Koutsoukos and C. G. Kontoyannis, *J. Cryst. Growth*, 1984, **69**, 367.
- 28 A. G. Xyla and P. G. Koutsoukos, *J. Chem. Soc., Faraday Trans. 1*, 1987, **83**, 1477.

Paper 2/05064A; Received 22nd September, 1992